

cient region it is possible to get an excellent superposition of the curves for the two temperatures by a single horizontal plus vertical shift. The matching process, which again appears unique, consists of a horizontal shift of 0.10 eV and a vertical shift factor of 1.7 (i.e., multiplying 77°K data by 1.7). This gave a superposition of curves from  $\sim 5 \times 10^3$  to  $\sim 0.5 \text{ cm}^{-1}$  (lower limit of data). The horizontal shift gives a temperature coefficient of band gap of  $-4.5 \times 10^{-4} \text{ eV}/^\circ\text{K}$ . The vertical shift is again of the order of magnitude predicted by theory.

#### ACKNOWLEDGMENTS

We are greatly indebted to L. Keifer and J. H. McTaggart for their painstaking work in the preparation of the samples. We should also like to thank A. G. Tweet for the Hall measurements on the thin samples. We have profited from discussion with E. O. Kane of the theoretical aspects of this work. We are indebted to H. Brooks for comments on the manuscript prior to publication.

*Note added in proof.*—Since the preparation of this manuscript, MacFarlane and Roberts [Phys. Rev. **97**, 1714 (1955); **98**, 1865

(1955)] have presented data for germanium and silicon in the low-absorption coefficient range (i.e.,  $\alpha$  less than  $100 \text{ cm}^{-1}$ ). Their data differ in detail from those presented here. The latter are, however, in very good agreement in the overlapping range with data previously presented.<sup>4,6</sup>

MacFarlane and Roberts analyze their data in terms of the indirect transition model of Hall, *et al.*,<sup>7</sup> taking the phonon contribution explicitly into account. This they do by plotting the square root of the absorption coefficient as a function of photon energy and decomposing the resultant curve into two straight line sections. The section at low energies is ascribed to a process in which a phonon is absorbed, the section at higher energies to one in which a phonon is emitted. From their data they estimate that the phonon required is characterized by a temperature of 260°K for Ge and 600°K for Si.

Our data do not show as obvious a resolution into two such linear sections when plotted after the manner of MacFarlane and Roberts. An analysis of our data in terms of vertical and horizontal shifts with temperature, as described in the body of our paper, would suggest phonons characterized by temperatures of  $\sim 300^\circ\text{K}$  for Ge and  $500^\circ\text{K}$  for Si. However, as Brooks has pointed out to us, there is a temperature dependence in the term  $(E_{c0} - E_{c(111)})^{-2}$  (see reference 7 for definitions) which appears in the theoretical expression for the absorption coefficient. This dependence is comparable to the temperature dependence explicitly expressed by the phonon population. Consequently, any analysis based solely on a phonon population effect is probably not too meaningful.

## Surface Barrier Analysis for Metals by Means of Schottky Deviations\*

D. W. JÜENKER

*University of Notre Dame, Notre Dame, Indiana*

(Received April 15, 1955)

The transmission coefficient for the mirror-image barrier at a metal surface is applied to the case of photoelectric emission. The distribution over which the coefficient is averaged is that given by Fowler for energies normal to the emitter surface, and is altered by the Schottky barrier lowering. The average differs from unity by an amount the major part of which is a periodic function of the accelerating field, giving a periodic deviation from the photoelectric Schottky effect which differs from the thermionic deviation only in amplitude. A refinement in the computation of the unaveraged periodic transmission coefficient brings the theory for thermionic deviations into agreement with that of Miller and Good. The improved form of the thermionic deviation is applied to experimental data to evaluate the complex reflection coefficient  $\mu$  characterizing the potential form in the immediate vicinity of the surface. The values of  $|\mu|$  so obtained for the highly refractory metals are of the order of 0.4, as compared with 0.2 predicted on the basis of the box model.

### I. INTRODUCTION

**E**LECTRONS emitted through a metallic surface into an accelerating field undergo reflection at the surface itself and at the maximum of the mirror-image barrier. The interference resulting from this double reflection manifests itself in periodic deviations from the Schottky effect.<sup>1</sup> In a previous publication,<sup>2</sup> there was formulated a transmission coefficient characteristic of the metallic barrier shape and suitable for the discussion of any emission process involving electrons

of low average escape energies. A particular application was made to the case of thermionic emission. In the present work, the parallel case of photoelectric emission will be considered. In the early stages of this work, it was found that the periodic part of the transmission coefficient could be expressed in better form.<sup>3</sup> The only effect of this refinement is to increase the theoretical amplitude of the periodic Schottky deviation; the basic conclusions found previously<sup>2</sup> remain unchanged. The revised transmission coefficient will be described here, and its effects on the interpretation of thermionic data will be discussed before applying it to the formulation of the photoelectric theory.

\* This research was sponsored by the U. S. Atomic Energy Commission.

<sup>1</sup> E. Guth and C. J. Mullin, Phys. Rev. **59**, 575 (1941); **59**, 867 (1941).

<sup>2</sup> Juenker, Colladay, and Coomes, Phys. Rev. **90**, 772 (1953).

<sup>3</sup> The author is indebted to Dr. Conyers Herring for pointing out the suitable process in a private communication.

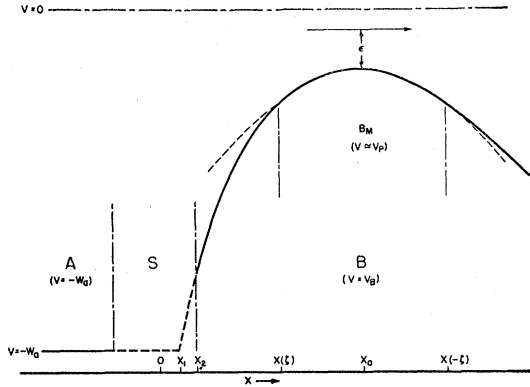


FIG. 1. Descriptive diagram of electronic potential energy  $v_s$  distance from the metal surface. An electron escaping with excess energy  $\epsilon$  passes from a nonreflecting region  $A$ , through a reflecting region  $S$  at the surface, into the mirror-image region  $B$ . Within  $B$  is a region  $B_M$ , including the barrier maximum at  $x_0$ , which is capable of reflecting electrons having low energy  $\epsilon$ . In region  $B_M$ , between  $x(\zeta)$  and  $x(-\zeta)$ , the mirror-image potential may be approximated as a parabola  $V_P$ , shown as a dashed curve. For the box model, described by the dashed curve in region  $S$ ,  $V_B$  and  $V_A$  are joined in a field discontinuity at  $x_1$ .

## II. REVISED TRANSMISSION COEFFICIENT

For a system of two plane parallel reflectors, the electron transmission coefficient for normal incidence may be written in terms of complex wave-reflection coefficients characteristic of the reflectors.<sup>2</sup> Letting these be  $\mu$  and  $\lambda$ , and assuming  $|\mu|^3 \ll 1$ , the transmission coefficient has the form

$$D = 1 - |(\lambda + \mu)/(1 + \lambda\mu^*)|^2 \simeq D_0 + D_1 + D_2, \quad (1a)$$

where

$$D_0 = 1 - |\lambda|^2, \quad (1b)$$

$$D_1 = -|\mu|^2[(1 - |\lambda|^2)^2 - 2|\lambda|^2(1 - |\lambda|^2)\cos 2\sigma], \quad (1c)$$

$$D_2 = 2|\mu||\lambda|(1 - |\lambda|^2)\cos\sigma, \quad (1d)$$

$$\sigma = \arg\lambda - \arg\mu + \pi. \quad (1e)$$

Such a doubly reflecting system is presented by the metallic surface barrier, shown in Fig. 1. In the region  $B$ , beyond some distance  $x_2$  outside the surface, an electron moves in a potential composed of the effects of its mirror image and the applied field, as given by

$$V_B = -(2x)^{-1} - x(2x_0^2)^{-1}, \quad (2)$$

where distances are in units of the first Bohr radius ( $a_0 = \hbar^2/mc^2 = 0.529$  Å) and  $V_B$  is in units of the hydrogen ionization potential ( $W_H = me^4/2\hbar^2 = 13.58$  eV). The field-dependence of  $V_B$  is embodied in the position  $x_0$  of the barrier maximum, given by  $x_0 = 3.587 \times 10^4 E^{-\frac{1}{2}}$  for the field  $E$  in  $v\text{-cm}^{-1}$ . In the vicinity of  $x_0$ , an electron having a low escape energy  $\epsilon$  has some probability of being reflected, in the case of positive  $\epsilon$ , or transmitted, for negative  $\epsilon$ . This region is designated  $B_M$  in Fig. 1, and is bounded at  $x(\zeta)$  and  $x(-\zeta)$ . Between  $x_2$  and  $x(\zeta)$  lies a comparatively nonreflecting

region, and in region  $A$ , in the metal's interior, one can assume a plane wave function to describe the electron. Separating  $A$  and  $B$  lies the reflecting region  $S$  brought about by the surface field.

The complex wave-reflection coefficients for the regions  $S$  and  $B_M$  have been evaluated<sup>2</sup> and represented by the symbols  $\mu$  and  $\lambda$ , respectively. For electrons incident on the barrier from region  $A$  one can arbitrarily assign to  $\mu$  and  $\lambda$  the following forms, which will prove convenient in subsequent manipulations:

$$|\mu| = \cos\Delta, \quad (3a)$$

$$\arg\mu = \pi + \phi - \Delta, \quad (3b)$$

$$|\lambda| = |\lambda_0|, \quad (4a)$$

$$\arg\lambda = \arg\lambda_0 + \left( \pi + \phi' - 2\Delta - 2 \int_{x_0}^{x_2} \kappa_B dx \right), \quad (4b)$$

where  $\kappa_B$  is the wave number of an electron moving in the potential given in (2). The quantities  $\phi$ ,  $\phi'$ , and  $\Delta$  depend on the barrier shape in region  $S$ . In (4), the quantity  $\lambda_0$  is the reflection coefficient to be attributed to the region  $B_M$  considered as an isolated reflector. Thus  $\arg\lambda_0$  represents the phase change suffered by an electron wave reflected in  $B_M$ . The integral term in (4b) corresponds to the phase accumulation of such a wave proceeding from  $x_2$  to its reflection in  $B_M$  and returning, and the quantity  $(\pi + \phi' - 2\Delta)$  may be interpreted as the phase change incurred in two opposite transits of region  $S$ . Then the quantity  $\sigma$  in (1e) describes the interference to the left of region  $S$  between a wave reflected in  $S$  and one reflected in  $B_M$ .

The evaluation of  $\lambda_0$  proceeds as follows: from (2),

$$\begin{aligned} \kappa_B &= [\epsilon + V_B(x_0) - V_B(x)]^{\frac{1}{2}} \\ &= [\epsilon + (x_0 - x)^2 / (2x_0^2 x)]^{\frac{1}{2}} \\ &= [4\beta\epsilon + z^2(1 - \beta^2 z^2 / x_0^2)^{-1}]^{\frac{1}{2}} / [4\beta]^{\frac{1}{2}}, \end{aligned} \quad (5a)$$

where

$$z = (x_0 - x) / \beta^{\frac{1}{2}} \quad (5b)$$

and

$$\beta = (x_0^3 / 2)^{\frac{1}{2}}. \quad (5c)$$

If one assumes the existence of a position  $x(\zeta)$  where  $z = \zeta$ , such that

$$|4\beta\epsilon| \ll \zeta^2 \ll x_0^2 / \beta,$$

then one can consider the potential in region  $B_M$  to be parabolic, with the corresponding wave function<sup>2</sup> (for a pure outgoing wave as  $x \rightarrow \infty$ )

$$\begin{aligned} \psi_P &\propto z^{-\frac{1}{2}} [(2\pi)^{\frac{1}{2}} / \Gamma(\frac{1}{2} - i\beta\epsilon)] \\ &\quad \times \exp[-\pi\beta\epsilon/4 - i(z^2/4 + \beta\epsilon \ln z - \pi/8)] \\ &\quad + z^{-\frac{1}{2}} \exp[-3\pi\beta\epsilon/4 + i(z^2/4 + \beta\epsilon \ln z - 3\pi/8)], \end{aligned}$$

while a WKB wave function satisfies (5a) for  $x_2 < x < x(\zeta)$ :

$$\psi_B = b_1 \kappa_B^{-\frac{1}{2}} \exp\left(i \int_{x_0}^x \kappa_B dx\right) + b_2 \kappa_B^{-\frac{1}{2}} \exp\left(-i \int_{x_0}^x \kappa_B dx\right).$$

The joining of  $\psi_B$  to  $\psi_P$  at  $x(\zeta)$  gives<sup>2</sup>

$$\lambda_0 = b_2/b_1 = (1 + e^{2\pi\beta\epsilon})^{-\frac{1}{2}} \exp i \left[ (C + \ln \zeta^2) \beta \epsilon + \zeta^2/2 + 2 \int_{x_0}^{x(\zeta)} \kappa_B dx - \pi/2 \right], \quad (6)$$

where  $C = (\gamma_E + 2 \ln 2) = 1.96$ ,  $\gamma_E$  being Euler's constant. Using (3b), (4b), and (6) in (1e), one has

$$\sigma = (C + \ln \zeta^2) \beta \epsilon + \zeta^2/2 + \pi/2 - \Delta + \phi' - \phi + 2 \int_{x_2}^{x(\zeta)} \kappa_B dx. \quad (7a)$$

Now, throughout the integration interval of the last term of (7a), the condition  $z^2 \geq \zeta^2 \gg |4\beta\epsilon|$  holds, so that  $\kappa_B$  may be expanded about  $\epsilon=0$ . Neglecting all but the first two terms, it becomes

$$\kappa_B = \kappa_0 + \epsilon/(2\kappa_0),$$

where  $\kappa_0 = \kappa_0(x) = \kappa_B(\epsilon=0)$ . Then, for  $x_2 \ll x_0$ ,

$$2 \int_{x_2}^{x(\zeta)} \kappa_B dx \simeq y - (8x_2)^{\frac{1}{2}} - \zeta^2/2 - (4 + \ln \zeta^2 - \ln y - \ln 12) \beta \epsilon, \quad (7b)$$

where

$$y = 4(2x_0)^{\frac{1}{2}}/3 = 357.1E^{-\frac{1}{2}} \quad (8)$$

for field  $E$  in v-cm<sup>-1</sup>. Replacing (7b) in (7a) and using  $\alpha = |\beta\epsilon|$ , one has

$$\sigma = \sigma_0 \pm g\alpha, \quad (9a)$$

which is the form arrived at in previous work.<sup>2</sup> Now, however,

$$\sigma_0 = (y + \pi/2) - \delta, \quad (9b)$$

$$\delta = \Delta + (8x_2)^{\frac{1}{2}} + (\phi - \phi'), \quad (9c)$$

$$g = C - 4 + \ln 12 + \ln y. \quad (9d)$$

The phase angle  $\delta$ , which is taken as characteristic of region  $S$ , has been changed only in formulation from the value given in reference 2. The explicit dependence on the position  $x_2$  has been included to point out that the surface reflecting region under investigation must take in all of the unknown territory between the limits of applicability of the constant interior potential and mirror-image law. However, the major contribution to the reflection cannot be made very far outside the surface, since it is found experimentally that  $\delta$  is not a function of applied field. The origin of the components of  $\delta$  is given in (3) and (4).

The value of  $g$  given in (9d) differs substantially from that given in Eq. (12c) of reference 2. The latter was found by numerical solution of the phase integral

$$\int_{x_2}^{x_0} \kappa_B dx = \int_{x_2}^{x_0} \kappa_0 dx + f(\alpha),$$

as a result of which  $g$  was considered a constant of the order of 5.3 over the effective range of  $\alpha$ . The present

value of  $g$ , in (9d), takes on values between 4.0 and 2.5 for fields ranging from 10 to 2000 kv-cm<sup>-1</sup>. It is preferable to the earlier form since its derivation is consistent with the other approximational methods employed in the evaluation of  $\lambda$ .

For the sake of comparison, one can evaluate  $|\mu|$  and  $\delta$  for the special case of the box model. For this example, the potential in region  $S$  takes on the particular shape shown by the dashed curve in Fig. 1. The mirror-image form is assumed valid beyond the point  $x_1$  where it crosses the average interior potential  $V_A = -W_a$ . For this case, the components of  $\mu$ , in (3), can be evaluated by joining at  $x_1$  a plane wave in region  $A$  to a WKB wave in region  $B$ . This procedure gives

$$\phi_c = \phi_c' = 2x_1\kappa_1 \simeq W_a^{-\frac{1}{2}}, \quad (10a)$$

$$\Delta_c = \cot^{-1} |\kappa_1'/4\kappa_1^2| \simeq \cot^{-1}(W_a^{\frac{1}{2}}/4), \quad (10b)$$

where  $\kappa_1 = \kappa_B(x_1) \simeq W_a^{\frac{1}{2}}$  and  $\kappa_1' = (d\kappa_B/dx)_{x_1} \simeq -W_a^{\frac{3}{2}}$ . Thus, using (3a) and (9c), and replacing  $x_2$  by  $x_1$ ,

$$|\mu|_c = \cos \Delta_c \simeq W_a^{\frac{1}{2}}(16 + W_a)^{-\frac{1}{2}}, \quad (11a)$$

$$\begin{aligned} \delta_c &= \Delta_c + (8x_1)^{\frac{1}{2}} \\ &= \cot^{-1}(W_a^{\frac{1}{2}}/4) + (W_a^{\frac{1}{2}}/4)^{-1}. \end{aligned} \quad (11b)$$

### III. THERMIONIC SCHOTTKY DEVIATION

The foregoing development changes the thermionic results of reference 2 only in the average of the transmission coefficient  $D_2$ .  $D_2$ , as stated in (1d), can be constructed from the parts given in (3), (4), (6), and (9), and is given in expanded form in Eq. (18), to follow. It must be averaged over the Maxwellian distribution

$$N_t(\alpha) = K_t e^{-2\pi B\alpha}, \quad (12)$$

where

$$\alpha = |\beta\epsilon|, \quad (13a)$$

$$B = (2\pi\beta kT)^{-1}, \quad (13b)$$

and where  $K_t$  is a constant of proportionality independent of  $\alpha$ . The averaging integration is straightforward, and results<sup>2</sup> in a convergent summation of terms periodic in  $\sigma_0$ . The summation is readily evaluated for given values of  $y = 357.1E^{-\frac{1}{2}}$ , providing numerical values for  $f_1(y)$  and  $f_2(y)$  in the relation

$$\langle D_2 \rangle_{av} = |\mu| B f_1(y) \cos[\sigma_0 + f_2(y)].$$

Such a procedure has been carried out for values of  $y$  in the range  $3\pi < y < 12\pi$  and it is found that  $f_2(y)$  varies from 0.6 by less than 0.1 radian over the whole range of  $y$ . The argument of the cosine is therefore essentially unchanged from its former value.<sup>2</sup>  $f_1(y)$  can be represented satisfactorily by the form

$$f_1(y) \simeq 5.1y^{-0.3},$$

so that the final average of  $D_2$  is

$$\langle D_2 \rangle_{av} \simeq 5.1y^{-0.3} |\mu| B \cos(\sigma_0 + 0.6). \quad (14)$$

The sizable contribution of electron tunneling near the barrier maximum is included in this expression.

Substitution of numerical values in  $B$ , as given in (13b), and multiplication by  $\log_{10} e$  transposes (14) to the periodic deviation  $F_2$  from the thermionic Schottky effect:

$$F_2 \simeq \log(I/I_0) - mE^{\frac{1}{2}} \simeq \log(1 + \langle D_2 \rangle_{Av}) \\ \simeq 4.9 \times 10^5 |\mu| T^{-1} \gamma^{-3.3} \cos(\gamma + 2.1 - \delta), \quad (15a)$$

where  $I_0$  is the zero-field current and  $m$  the Schottky slope, and where  $T$  is the Kelvin temperature.  $\delta$  is described generally in (9c) and for the special case of the box model in (11b). The small nonperiodic deviation  $F_1$  has been neglected in (15a). By way of comparison, the result found by Miller and Good<sup>4</sup> contains a cosine argument nearly identical with that of (15a), and an amplitude which can be stated approximately as

$$|F_2|_{MG} = 4.6 \times 10^5 |\mu| T^{-1} \gamma^{-3.2}. \quad (15b)$$

Since the periodicity in experimental deviation data has been found to agree accurately with that of (15a), such data have been analyzed to obtain values for  $\delta$  and  $|\mu|$ . Equation (15a) differs from the earlier value of  $F_2$  given in reference 2 only in amplitude. Therefore the present revised form yields the same result with respect to the phase  $\delta$ : experimental values for  $\delta$  for the highly refractory metals are smaller by a quarter period than the values calculated from (11b), indicating the existence of a potential shape in the region  $S$  of Fig. 1 different from the field discontinuity presented by the box model. Experimental values for  $|\mu|$ , on the other hand, are increased in magnitude by the revision of  $F_2$ . Hence, the values of  $|\mu|_x$  cited in Table II of reference 2 must be replaced by values found from (15a) above, namely,

$$|\mu|_x = 2.06 \times 10^{-6} A_m T \gamma_m, \quad (16)$$

where  $A_m$  and  $\gamma_m$  are the amplitude and field position of the  $m$ th extremum of the experimental  $F_2$  deviation. The values obtained for tungsten, tantalum, and molybdenum are given in Table I.

TABLE I. Amplitude analysis for thermionic data on tungsten, tantalum, and molybdenum. Here,  $\gamma_m$  indicates the extrema analyzed, italics designating maxima.  $|\mu|_x$  is computed from Eq. (16); the largest and smallest values found for  $|\mu|_x$  are given. The corresponding theoretical value  $|\mu|_c$  is calculated for the box model by converting the value of  $W_a$  shown in the table to Rydberg units and substituting in Eq. (11a).

	Tungsten Seifert, Phipps <sup>a</sup>	Tantalum Munick, LaBerge, Coomes <sup>b</sup>	Molybdenum Brock, Houde, Coomes <sup>c</sup>
$\gamma_m$	21.9, 25.3	24.9, 27.9, 31.1	25.6, 28.7
$ \mu _x$	0.39–0.46	0.35–0.45	0.30–0.42
$W_a$	10.3 ev	9.3 ev	10.2 ev
$ \mu _c$	0.22	0.21	0.22

<sup>a</sup> R. L. E. Seifert and T. E. Phipps, Phys. Rev. **56**, 652 (1939).

<sup>b</sup> Munick, LaBerge, and Coomes, Phys. Rev. **80**, 887 (1950).

<sup>c</sup> Brock, Houde, and Coomes, Phys. Rev. **89**, 851 (1953).

<sup>4</sup> S. C. Miller and R. H. Good, Phys. Rev. **92**, 1367 (1953).

#### IV. PHOTOELECTRIC SCHOTTKY DEVIATION

The transmission coefficient  $D$  will be applied to the case of surface photoelectric emission in the following development. The assumptions of Fowler<sup>5</sup> will be used: (a) that the number of electrons in a metal "available" for photoelectric emission is equivalent to the number whose energy component normal to the surface, augmented by the illumination energy  $h\nu$ , is sufficient to surmount the surface barrier; and (b) that the probability that one of these "available" electrons will be excited by illumination near the threshold is independent of energy.

For photoelectric emission, therefore, the equivalent of the Maxwellian distribution in the thermionic case is a Fermi distribution which has been integrated over the two directions parallel to the surface. This can be written

$$N_p(\epsilon) = K_p \ln[1 + \exp(\chi' - \epsilon/kT)], \quad (17)$$

where

$$\chi' = h(\nu - \nu_0')/(kT) \\ = [h(\nu - \nu_0) - V_B(x_0)]/(kT) \\ = [h(\nu - \nu_0) + x_0^{-1}]/(kT),$$

$\epsilon$  is the electron energy relative to the barrier maximum as shown in Fig. 1,  $K_p$  is a constant of proportionality approximately independent of  $\epsilon$ , and  $h\nu_0$  is the zero-field threshold.

The transmission coefficient given in (1) can be expressed as a function of field and energy by inserting the values of  $\lambda$  and  $\mu$  from (3), (4), (6), and (9). It can then be expanded as follows, with  $\alpha = |\beta\epsilon|$ :

$$D_0 = \frac{1}{2}(1 \pm 1) \pm \sum_{n=1}^{\infty} (-1)^n e^{-n2\pi\alpha}, \quad (18a)$$

$$D_1(m) = -|\mu|^2 \left[ \frac{1}{2}(1 \pm 1) - \sum_{n=1}^{\infty} (-1)^{n+1} (n \pm 1) e^{-n2\pi\alpha} \right], \quad (18b)$$

$$D_1(p) = 2|\mu|^2 \sum_{n=1}^{\infty} (-1)^{n+1} n e^{-n2\pi\alpha} \cos 2(\sigma_0 \pm g\alpha), \quad (18c)$$

$$D_2 = 2|\mu| \sum_{n=0}^{\infty} (-1)^n \frac{\Gamma(n + \frac{3}{2})}{\Gamma(\frac{3}{2})\Gamma(n+1)} \\ \times e^{-a_n\alpha} \cos(\sigma_0 \pm g\alpha), \quad (18d)$$

where  $D_1 = D_1(m) + D_1(p)$ ,  $a_n = 2\pi[n - (\pm\frac{1}{4} - \frac{3}{4})]$ , and where the plus-or-minus signs indicate the sign of  $\epsilon$ .  $\sigma_0$  and  $g$  have been given in (9). For the extreme field  $E = 500$  kv-cm<sup>-1</sup>,  $2\pi\alpha$  exceeds unity for  $|\epsilon|$  greater than about 0.008 ev. Therefore, for purposes of averaging (18) over the distribution (17),  $|\epsilon|$  may be considered small compared with  $kT$ , even at room temperature. It is also simpler to work with  $h(\nu - \nu_0)$  of such a magnitude that  $\chi'$  is large compared with  $\exp(-\chi')$ . At room temperature this is normally

<sup>5</sup> R. H. Fowler, Phys. Rev. **38**, 45 (1931).

satisfied with frequencies such that  $h(\nu - \nu_0) > 0.05$  ev. For this case, the logarithmic term in (17) may be expanded, retaining

$$N_p(\alpha) \simeq -K_p(\pm 2\pi B\alpha - \chi'), \quad (19)$$

where the plus and minus again refer to the sign of  $\epsilon$ .

The average transmission coefficient is defined by

$$\langle D \rangle_{Av} = \frac{\int_0^\infty D_+(\alpha) N_+(\alpha) d\alpha + \int_0^\infty D_-(\alpha) N_-(\alpha) d\alpha}{\int_0^\infty N_+(\alpha) d\alpha}, \quad (20)$$

where the subscripts indicate the quantities in (18) and (19) evaluated for the corresponding energy ranges, the second term in the numerator being the tunnelling contribution. The denominator of (20) must be found

from a two-part integration,<sup>5</sup> using the original form of the distribution given in (17). To a sufficient approximation it is

$$\int_0^\infty N_+(\alpha) d\alpha = \beta \int_0^{\chi' kT} N_p(\epsilon) d\epsilon + \beta \int_{\chi' kT}^\infty N_p(\epsilon) d\epsilon \simeq K_p P (4\pi B)^{-1}, \quad (21)$$

where

$$P = \frac{1}{3}\pi^2 + \chi'^2, \quad (22)$$

and  $B$  is given in (13b). The averages of (18) can be found by applying (19), (20), and (21). Neglecting terms smaller than  $B^2/P$  and  $|\mu|^2$ , the results are

$$\langle D_0 \rangle_{Av} \simeq 1 + (\pi B)^2 (3P)^{-1}, \quad (23a)$$

$$\langle D_1(m) \rangle_{Av} \simeq -|\mu|^2 (1 - 2\chi' B P^{-1}), \quad (23b)$$

$$\langle D_1(p) \rangle_{Av} \simeq C_1 |\mu|^2 \chi' B P^{-1} \cos(2\sigma_0 - \theta_1), \quad (23c)$$

$$\langle D_2 \rangle_{Av} \simeq C_2 |\mu| \chi' B P^{-1} \cos(\sigma_0 + \theta_2). \quad (23d)$$

The quantities  $C_1$ ,  $C_2$ ,  $\theta_1$ , and  $\theta_2$  have been evaluated for values of  $y = 357.1E^{-1}$  in the practical field range, in the manner which has been described for the thermionic case. They have been found to fit the following relationships:

$$C_1 \simeq 6.16y^{-0.64}; \quad \theta_1 \simeq \tan^{-1}[14y^{-2.9}(\chi' kT)^{-1}]; \\ C_2 \simeq 10.12y^{-0.33}; \quad \theta_2 \simeq 0.6.$$

The photoelectric emission in an accelerating field should follow the relationship:

$$I = I_0 [P \langle D \rangle_{Av}] / [P_0 \langle D(0) \rangle_{Av}], \quad (24)$$

where  $\langle D \rangle_{Av}$  is the sum of the averaged coefficients in (23), and where  $I_0$ ,  $P_0$ , and  $\langle D(0) \rangle_{Av}$  are the zero-field quantities. From (22) and (23), the latter two are

$$P_0 = \frac{1}{3}\pi^2 + [h(\nu - \nu_0)/(kT)]^2, \quad \langle D(0) \rangle_{Av} = 1 - |\mu|^2,$$

Discarding terms in  $|\mu|^3$ , one may write (24) in terms of the first-order photoelectric Schottky current  $I_1$ :

$$\begin{aligned} (I - I_1)/I_1 &\simeq \langle D \rangle_{Av} - \langle D(0) \rangle_{Av} \\ &\simeq B(\pi^2 B + 6\chi' |\mu|^2) / (3P) \\ &\quad + C_1 |\mu|^2 \chi' B P^{-1} \cos(2\sigma_0 - \theta_1) \\ &\quad + C_2 |\mu| \chi' B P^{-1} \cos(\sigma_0 + \theta_2) \\ &= \Phi_1 + \Phi_2' + \Phi_2, \end{aligned} \quad (25)$$

where  $I_1 = I_0 P / P_0$ . The monotonic  $\Phi_1$ , and  $\Phi_2'$ , which is periodic in  $2\sigma_0$ , have amplitudes less than 10% of that of  $\Phi_2$ , even for high fields and illumination near the threshold. The quantity  $I_0/P_0$  depends on the quantum efficiency of the surface and the intensity of illumination, and contains the factor  $(kT)^2$ . Hence, ideally,  $I_1$  is given by the proportionality<sup>1</sup>

$$I_1 \propto \frac{1}{3}(\pi kT)^2 + [h(\nu - \nu_0) + 48.3y^{-2}]^2.$$

However, due principally to the patch effect,  $I_1$  probably will be an empirical curve-fit in practice, and  $\Phi_1$  will be inseparable from experimental data.

In terms of the field parameter  $y$ , as given in (8), and  $kT$  and  $h\nu$  in electron volts, and with the values of

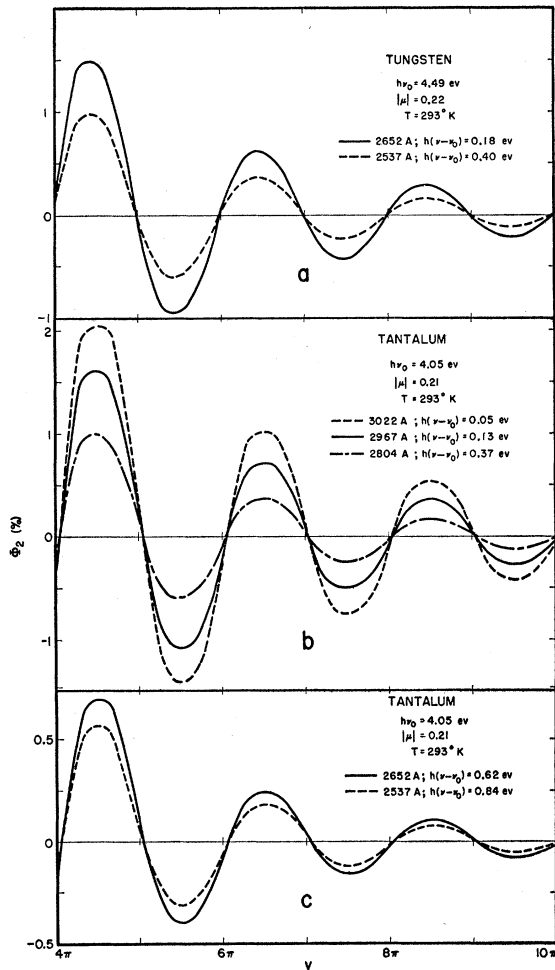


FIG. 2. The periodic deviation  $\Phi_2$  from the photoelectric Schottky effect.  $\Phi_2$  is plotted in percent as a function of  $y = 357.1E^{-1}$ , as given in Eq. (26b). The curves in (a) are for tungsten, and those in (b) and (c) are for tantalum; all are for room temperature, with illumination wavelengths corresponding to the more useful lines of the mercury spectrum. Note the doubled ordinate scale in (c).

$C_1$ ,  $C_2$ , and  $\theta_2$  included,  $\Phi_2'$  and  $\Phi_2$  are

$$\Phi_2' = \frac{126 |\mu|^2 y^{-3.6} \{h(\nu - \nu_0) + 48.3y^{-2}\}}{\{\frac{1}{3}(\pi kT)^2 + [h(\nu - \nu_0) + 48.3y^{-2}]^2\}} \times \cos[2y + \pi - \theta_1(y, \nu) - 2\delta], \quad (26a)$$

$$\Phi_2 = \frac{208 |\mu| y^{-3.3} \{h(\nu - \nu_0) + 48.3y^{-2}\}}{\{\frac{1}{3}(\pi kT)^2 + [h(\nu - \nu_0) + 48.3y^{-2}]^2\}} \times \cos[y + 2.1 - \delta]. \quad (26b)$$

$\Phi_2$  comprises almost the entire deviation from the photoelectric Schottky effect; it is the counterpart of the periodic deviation  $F_2$  in the thermionic case [see Eq. (15a)]. It is represented graphically in Fig. 2 for tungsten and tantalum, using the box model values  $|\mu|_e$  for  $|\mu|$  [see Table I and Eq. (11a)] and the threshold values<sup>6</sup> 4.05 eV for tantalum and 4.49 eV for tungsten.

## V. CONCLUSIONS

### A. Revised Thermionic Theory

The use of the revised transmission coefficient introduces no change in the conclusions reached in previous work,<sup>2</sup> other than the following additional remarks:

There is a striking similarity between the value of the thermionic Schottky deviation as determined in the present work with the revised transmission coefficient, and that found by Miller and Good.<sup>4</sup> The latter theory was formulated by means of a refined WKB approximations method but, as in the present case, a parabolic potential form was assigned to the barrier maximum. Therefore, although the experimental values for  $|\mu|$  given in Table I may be real, suspicion has not been completely removed from the parabolic approximation as being the cause of their apparently excessive magnitudes.

With regard to these values of  $|\mu|_x$ , it is to be noted that essentially external factors such as patch effect or surface irregularities would tend to give rise to mutually destructive Schottky deviations, resulting in low apparent values of  $|\mu|$ , rather than the high magnitudes actually observed. The presence of a third reflecting layer, such as one might suppose to exist in the case of a uniformly contaminated surface, would likewise lead to low measurements of  $|\mu|$  under ordinary circumstances.

It has been the practice throughout the present computations to neglect terms in  $|\mu|^3$  or higher order as they occur. This approximation is justified for  $|\mu| \sim 0.2$ , and appears to be generally satisfactory even for values of  $|\mu|$  near 0.4, since the terms in question usually occur in combination with other small quantities. However, in computing the final theoretical form of the periodic deviation in both the thermionic

and photoelectric cases, the approximation

$$\frac{[\langle D(0) \rangle_{Av} + \langle D_2 \rangle_{Av}]/\langle D(0) \rangle_{Av}}{= [1 - |\mu|^2 + \langle D_2 \rangle_{Av}]/[1 - |\mu|^2]} \approx 1 + \langle D_2 \rangle_{Av}$$

has been used, in keeping with the prior practice. In this instance,  $|\mu|^3$  is not necessarily negligible in comparison with unity, but the retention of higher order terms lowers the values of  $|\mu|_x$  in Table I by only  $\sim 15\%$ .

The agreement in phase and period of the periodic deviation  $F_2$  found here and in reference 2, with that of Miller and Good, is reassuring. There was some doubt whether the ordinary WKB wave function could be validly applied at the barrier corner  $x_1$  of the box model. Were such doubt well founded, it would seem that the improvement in method employed by Miller and Good should result in a phase shift in  $F_2$ ; such a shift is not found.

### B. Photoelectric Theory

A comparison of (26b) with (15a) shows the phase and period of the thermionic and photoelectric deviations to be identical. The amplitudes are also essentially the same in form; due to the different energy distributions involved, the thermionic form has a  $T^{-1}$ -dependence while the photoelectric amplitude can be thought of as depending on  $(h\nu - h\nu_0)^{-1}$ , neglecting the temperature "tail" of the Fermi distribution.

It has been noted here and previously<sup>2</sup> that the evaluation of  $|\mu|$  from experimental thermionic data is subject to some ambiguity, due not only to theoretical deficiencies, but also to the influence of patch effects on the data themselves. Even greater ambiguity will occur in the photoelectric case since to these same difficulties is added that of defining a value for  $h(\nu - \nu_0)$ , especially for a patchy emitter. This condition could be improved by a working knowledge of the first-order behavior of photoelectric emission in the Schottky field region.

Since  $|\mu|$  should be independent of emission mechanism, one can expect experimental deviation amplitudes about twice those graphed in Fig. 2, as in the thermionic case, barring the aforementioned difficulty in defining  $h(\nu - \nu_0)$ . There is no apparent reason to expect phase or period different from those found for thermionic deviations, i.e., experimental curves shifted to the left of the theoretical curves of Fig. 2 by about a quarter period. Experimental data on photoelectric deviations<sup>7</sup> are not yet available in the quantity which makes possible analysis of the counterpart thermionic results. In principle, however, the photoelectric method has obvious advantages: a broader range of subject materials, and the possibility of examining discrete portions of a surface.

The author gratefully acknowledges the helpful criticism and suggestions of Dr. E. A. Coomes and Dr. R. H. Good.

<sup>6</sup> C. Herring and M. H. Nichols, Revs. Modern Phys. **21**, 185 (1949), Table IV.

<sup>7</sup> Buder, Ruddick, and Weber, Phys. Rev. **91**, 561 (1953).